THE ASTRONOMICAL JOURNAL, 120:2569–2578, 2000 November

SPECTRAL ENERGY DISTRIBUTION AND ABUNDANCES OF NGC 288 STARS

ALFRED BING-CHIH CHEN,[1] WEAN-SHUN TSAY,[2] AND WEN-SHU TSAI
Institute of Physics and Astronomy, National Central University, 38 Wu-Chan li, Chung-li, 32054 Taiwan; alfred@joule.phy.ncu.edu.tw, tsay@virgo.phy.ncu.edu.tw, ccl@virgo.phy.ncu.edu.tw

AND

PHILLIP K. LU[2,3]
Department of Astronomy, Yale University, P.O. Box 208101, New Haven, CT 06520; lup@astro.yale.edu, lu@wcsu.ctstateu.edu
Received 2000 April 25; accepted 2000 July 5

ABSTRACT

NGC 288, an intermediate Population II globular cluster located near the south Galactic pole, has a dominant blue horizontal branch, intermediate metallicity, and age about 15 Gyr. It has been investigated in a number of studies using spectrophotometric techniques. We present here new spectral energy distributions (SEDs) of bright stars in NGC 288 constructed using 12 of the BATC (Beijing Arizona Taipei Connecticut) 15 intermediate-band filter systems. Using Kurucz models, we have estimated reliable effective temperatures for stars and $[\mathrm{Fe/H}] = -1.24 \pm 0.04$. Using theoretical isochrones that Worthey has calculated for our filter set, we obtain a distance modulus of $m-M = 14.57 \pm 0.07$ for this cluster. The purpose of this study is to establish a stellar SED data bank by using cluster stars of different age, temperature, abundance and surface gravity. The SEDs for the stars in NGC 288 form part of this data bank, which will be used for future studies of objects in Selected Area fields.

Key words: globular clusters: general — globular clusters: individual (NGC 288) — stars: evolution — stars: fundamental parameters — methods: statistical

1. INTRODUCTION

The observational objective of the Beijing Arizona Taipei color (BATC) survey is to obtain accurate spectral energy distributions (SEDs) of all objects — stars, galaxies, active galactic nuclei (AGNs), and quasi-stellar objects (QSOs)— found in 500 selected 1 deg^2 fields using a 0.6–0.9 m Schmidt telescope at the Xing Long Observing Station of the Beijing Astronomical Observatory (BAO). The scientific goals of the BATC survey have been detailed elsewhere (Fan et al. 1996; Lu et al. 1997; Zheng et al. 1999; Deng et al. 1999). The present paper is part of an effort both to obtain complementary calibration data for the BATC survey and to use the BATC filter system to do further Galactic structure studies. The main purpose of the present study is to obtain a set of accurate stellar SEDs for red giant branch, blue horizontal branch, and asymptotic giant branch stars in the globluar cluster NGC 288. We will then compare these SEDs with observational evolutionary tracks of globular clusters, as well as with the stellar atmosphere models of Kurucz (1993). These well-established SEDs will then be used to calibrate other Selected Area and low-latitude fields in a study of galactic structure (Lu 1989, 95; Lu 1991, 33; Lu 1993, 19; Tsay et al. 1997).

Briefly, the BATC filter system (Fan et al. 1996; Zheng et al. 1999; Deng et al. 1999) consists of 15 filters of bandwidths 150–350 Å that cover the wavelength range 3360 to 9745 Å. A clear advantage of this system over most other filter systems is that it avoids the brightest, most variable near-IR night-sky emission lines. Several sets of this filter system are now available among the member institutions in the BATC consortium for studies at various sites, including Cerro Tololo International Observatory, Mt. Stromlo Observatory in Australia, Steward Observatory in Arizona, and Lu-lin Observatory in Taiwan. However, the primary BATC program observations are still carried out using the BAO Schmidt telescope at the Xing Long station of the BAO in China.

The BATC survey is calibrated on an absolute flux scale using Oke & Gunn (1983) spectrophotometric standards as primary calibrators. To supplement these primary flux standards for the present study, we have used secondary stellar standards from the studies of Gunn & Stryker (1983) and Clampitt & Burstein (1997) here. Secondary calibrators were also established based on our own observations (Lu et al. 1997) for NGC 288 and other related Selected Area (SA) fields. Comparison between the current observations and those reported elsewhere shows good agreement.

The SEDs of standard stars of all spectral types determined by the BATC filter system permit a clear distinction in stellar temperature, which in turn can provide rapid spectral classification for stars and identification of galaxies and QSOs to a limiting magnitude of $V \sim 21$ in our data (Lu, Tsay, & Chen 1999, 3). The final aim of the present study is to develop a fiducial set of SEDs with different temperature, age, surface gravity, and abundance using globluar cluster and open cluster stars. The parameters of these SEDs refer to stars that are on the main sequence (MS), red giant branch (RGB), asymptotic giant branch (AGB), horizontal branch (HB) and blue horizontal branch (BHB) of this cluster.

NGC 288 is one of the most prominent objects near the south Galactic pole and has been included in a spectro-

[1] Visiting Student, Cerro Tololo Inter-American Observatory, which is operated by the Association of Universities for Research in Astronomy, Inc., under cooperative agreement with the National Science Foundation.
[2] Visiting Astronomer, Cerro Tololo Inter-American Observatory, which is operated by the Association of Universities for Research in Astronomy, Inc., under cooperative agreement with the National Science Foundation.
[3] Visiting Astronomer, Kitt Peak National Observatory, National Optical Astronomy Observatories, operated by the Association of Universities for Research in Astronomy, Inc., under cooperative agreement with the National Science Foundation.

photometric survey using the Strömgren photometric system and 2DF spectroscopy in a study of the galactic gravitational force K_z (Lu 1989, 95; Lu 1993, 19). Astrometry of this cluster has been done with the Yale Southern Proper Motion survey by Platais et al. (1998), and it has little Galactic reddening.[4] NGC 288 is one of the most frequently studied globular clusters that exhibits the so-called "second parameter" effect: it has a clearly defined BHB but a relatively high metallicity ([Fe/H] $\simeq$ 1.24; Harris catalog[4]) and old age (14.85 Gyr; Alcaino, Liller, & Alvarado 1997). NGC 362 and NGC 288 are often referred to as one of the classical "second-parameter" pairs, as they are similar in metallicity but different in HB morphologies (Lee, Demarque, & Zinn 1990; Stetson, Vandenberg, & Bolte 1996). A related study has indicated that this cluster is in retrograde orbital motion (Guo et al. 1993). Such an orbit indicates that our own Galaxy was very clumpy and turbulent in its initial phase of formation (van den Bergh & Hesser 1993).

2. OBSERVATION AND ANALYSIS

Two telescopes at Cerro Tololo Inter-American Observatory (CTIO) were used for this study. The 0.9 m CTIO telescope was used with the CF/CCD, which consists of a 2K × 2K chip yielding a field of view of 13.5 × 13.5 with an angular resolution of 0.″39 pixel^{-1}. This configuration was used with the BATC filter set to observe 13 open and globular clusters of various ages and abundance in LMC and SMC, together with observations of stars in the Hyades, Presepae, M67, and NGC 288. The Yale l m telescope was used with the automated single-channel aperture photometer (ASCAP) to obtain BATC filter observations of 14 bright SED standards selected from Gunn & Stryker (1983) and Clampitt & Burstein (1997), as well as other secondary standards stars in NGC 288, SA 92, SA 95, and M67 fields. Three secondary standard stars, 6053c, 6054d, and 6048x (Lu, Miller, & Platt 1992, 95) in NGC 288 were used to perform the SED zero-point shift in this study. A detailed discussion of ASCAP observations and calibrations for these data will be presented elsewhere by P. Lu. Only the CCD observations are discussed in this paper.

Because of the very low quantum efficiency of the CF/CCD at the bluest and reddest ends of the ground-based accessible spectrum, three BATC filters were not used ($m1$, 3360 Å; $m2$, 3890 Å, and $m15$, 9745 Å). Table 1 lists the observing log of NGC 288 using the 0.9 m telescope at CTIO in 1996 November and the corresponding central wavelength of various bandpasses, from which the stellar SEDs presented here were derived.

Preliminary reductions of the CCD frames, including bias, dark subtraction, and field flattening, were carried out with the standard CCD reduction package at CTIO. Instrumental magnitudes were measured using the DAOPHOT II stellar photometric reduction package of Stetson (1987), during which bad-pixel corrections were made. In general, more than 25 stars among the outer portions of NGC 288 were selected for fitting point-spread functions (PSF) for each BATC filter image. Sources of photometric error include photon statistics of star and sky, readout noise, random and systematic errors from bias subtraction and flat-fielding, hot and warm pixels, probable nonlinearity of the CCD, and the PSF fitting and calibration of standard stars in the reduction pipeline. The analysis package DAOPHOT II yields the theoretical prediction of the error based on the sky and stellar photon statistics and tries to estimate the error from PSF fitting. The overall photometric error distributions for all bandpasses are shown in Figure 1, and it is rather clear that there are no significant distinctions among the bandpasses; thus we can conclude that the overall absolute photometric zero-point accuracy for the data discussed here is 0.06 mag for stars brighter than 19th magnitude in most filters.

The final tables consist of IDs, relative positions in the field, photometry, and parameters derived from the Kurucz model (see § 2.1) for those stars for which $m4 < 18$. They and the finding charts can be retrieved from our web site.[5]

TABLE 1

OBSERVING LOG OF NGC 288 IN 1996 NOVEMBER

Filter	λ_c (Å)	Exposure (s)	Air Mass	Time 1996 Nov 25 (UT)
$m3$	4210	300	1.002	01:20:32
$m4$	4550	300	1.015	02:00:51
$m5$	4920	300	1.002	01:14:34
$m6$	5270	300	1.019	02:06:45
$m7$	5750	300	1.008	00:50:17
$m8$	6070	300	1.024	02:12:47
$m9$	6660	300	1.005	00:56:28
$m10$.....	7050	300	1.031	02:20:46
$m11$.....	7490	300	1.004	01:02:32
$m12$.....	8020	300	1.038	02:26:58
$m13$.....	8480	300	1.003	01:08:29
$m14$.....	9190	300	1.044	02:32:58

2.1. *Spectral Energy Distributions versus Model Predictions*

Three secondary SED standard stars were observed using the Yale 1 m telescope and ASCAP photometer (Lu et al. 1997), permitting an overall zero-point adjustment for all objects in the NGC 288 field. Equally important, we obtain verification of the accuracy of our SEDs by comparing our observations with the stellar models of Kurucz (1993). We establish the relative accuracy of our observations by comparing the SEDs of the hottest stars in our sample—BHB stars—with the Kurucz models. To do so we adopt a procedure of selecting four small sections in the BHB region (see Table 2) in a way that the range in mean $m4-m7$ color and mean $m7$ in each section is less than 0.1 mag. The average color and magnitude in these four sections and their mean SEDs are then compared with the Kurucz theoretical SEDs, resulting in an average $1-\sigma$ accuracy, model

[4] See W. E. Harris, Catalog of Parameters for Milky Way Globular Clusters (June 1999): http://physun.physics.mcmaster.ca/Globular.html.

[5] See http://www.astro.ncu.edu.tw/tsay/ngc288.

TABLE 2

MEAN MAGNITUDE AND COLOR OF THE FOUR GROUPS

$m7$	$m4-m7$	Number	S
15.38.....	−0.14	6	0.022
15.59.....	−0.21	4	0.020
15.96.....	−0.27	13	0.020
16.22.....	−0.30	8	0.028

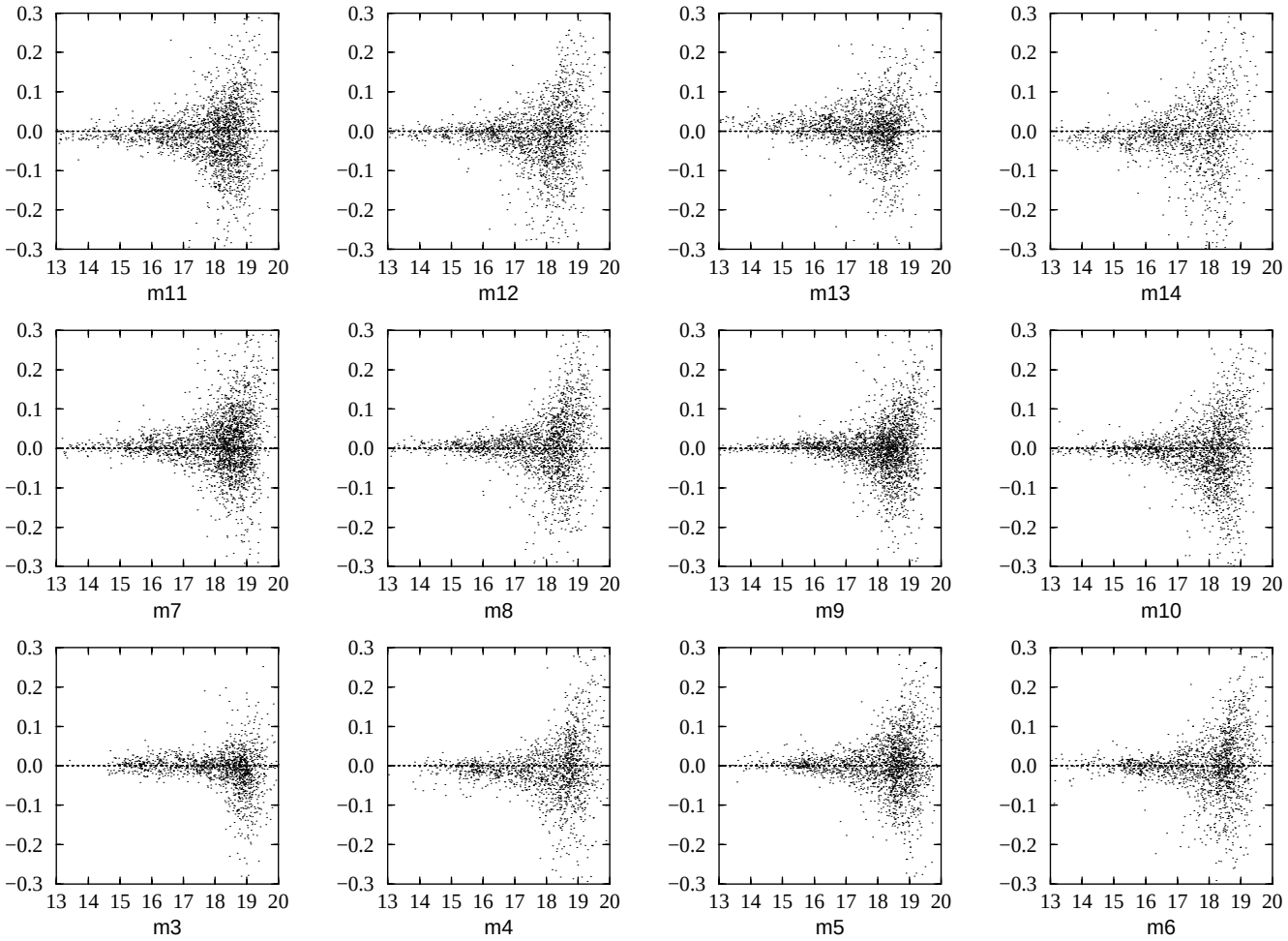

FIG. 1.—S vs. magnitude $m7$ photometric precision in 12 bandpasses. The magnitude errors derived from IRAF/DAOPHOT II and the deviations of calibration are included and plotted on the Y-axis.

to observation, of 0.023 mag. Comparison with similar tests using RGB and AGB stars yields consistent results.

The ranges chosen for the Kurucz models are effective temperature, $T_{\rm eff}$, between 3500 K and 50,000 K in intervals of 250 K, abundances, [Fe/H], between $+1$ and -5 in increments of 0.5, and surface gravities (log g) between 0 and 5 in increments of 0.5. About 7600 synthetic spectral types fall within these parameter ranges, providing a suitable number with which to fit our data.

The criteria of best fit between observed SED and Kurucz model is given by

$$S = \sqrt{\frac{\sum (m_i - M_i)^2}{n - 1}},$$

where m_i is the observed magnitude and M_i is the theoretical magnitude in filter i and n is the number of bandpasses in the fit (not all stars are observed in all bandpasses used).

The best fit would yield the smallest value of S, or the best-matched SED shapes between observed SEDs and the theoretical ones. Figure 2 shows S versus $m4$ after optimization. Of course, the amplitude of the standard deviation S is a function of apparent magnitude, becoming larger with fainter magnitudes. After some experimentation, only the SEDs of stars with $m4 < 18$ were selected for

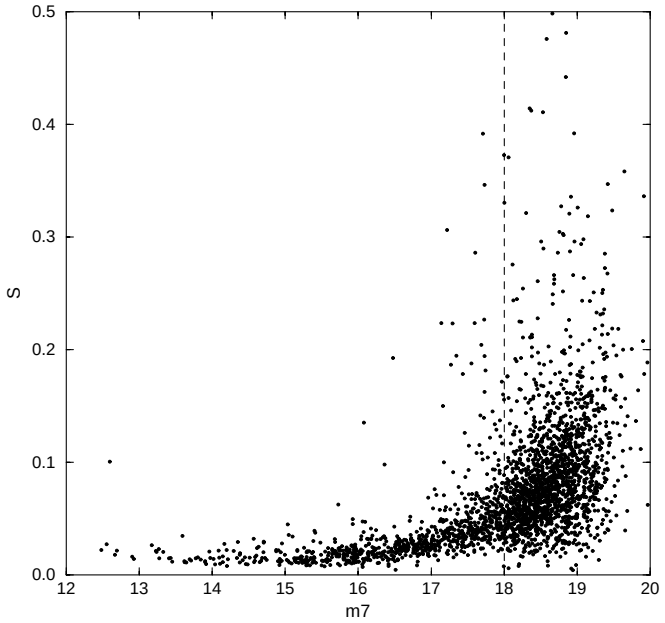

FIG. 2.—S vs. magnitude $m7$ after SED optimization for all objects. Based on this relationship, we have selected stars with $m7 < 18$ for further analysis.

further study. As our data set covers only the bright post–main-sequence stars in NGC 288, surface gravity differences among these stars are comparable to the resolution of the Kurucz models (0.5 dex), and hence the model comparsion conveys little gravity information. Therefore we will concentrate on abundance and effective temperature in the following sections.

The reliability of our abundance and effective temperature estimates can be checked by direct comparison with the spectroscopic determinations of Caldwell & Dickens (1988) and Pilachowski & Sneden (1983). Such a comparison is made in Table 3 for six RGB stars in common with these other studies. There is excellent agreement on temperature, indicating that the SED fit is very sensitive to temperature. Though only six commonly observed bright RGB stars were found and adapted in the comparison, the effective temperature was determined from the photometric data in a wide spectral range through SED fitting; thus it is possible to provide more accurate temperatures than traditional photometric methods for BHB and AGB stars. Our determination of [Fe/H] for these six RGB stars is systematically less metal-rich than the spectroscopic observations, but most values are still within the Kurucz model step size (0.5 dex) of the spectroscopic [Fe/H]. The coarse [Fe/H] can provide only a rough estimate of individual stellar abundances, but we have the advantage of being able to use many stars to obtain a more accurate estimate for the cluster as a whole.

The SEDs of four randomly selected RGB, AGB, and BHB stars are plotted with their corresponding theoretical curves in Figure 3. Note that an arbitrary shift is applied to each object for convenient comparison, since the display

TABLE 3

TEMPERATURE AND ABUNDANCE COMPARISONS

Star[a]	V	$(B-V)$	$T_{\rm eff}$[b]	$T_{\rm eff}$[c]	$T_{\rm eff}$[d]	[Fe/H][b]	[Fe/H][c]	[Fe/H][d]
358/78	12.92	1.42		4150	4000		−1.11	−1.0
481/ 77	13.12	1.34	4120	4300	4250	−1.05	−0.90	−1.5
902/194	13.10	1.31		4300	4250		−0.96	−1.5
1829/ 96	12.74	1.51		4100	4000		−1.19	−1.5
2294/213.....	13.00	1.32		4100	4250		−0.74	−1.0
3985/ 48	13.40	1.26	4230		4250	−0.90		−1.5

[a] BATC, Alcaino & Liller 1980.
[b] Caldwell & Dickens 1988.
[c] Pilachowski & Sneden 1983.
[d] BATC: this work.

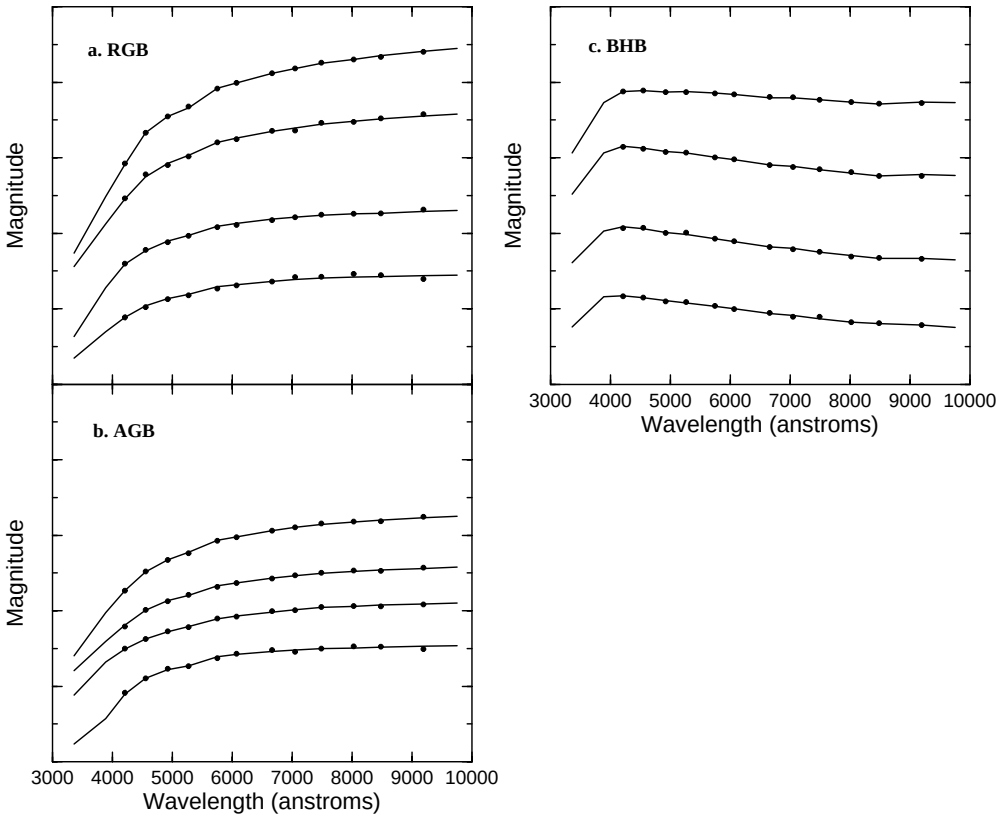

FIG. 3.— SEDs of four stars randomly selected from each of the RGB, AGB, and BHB subsets of our data compared with the Kurucz models. The circles are the observations plotted at the effective wavelengths of the BATC filters. The line is the best-fit theoretical SED from Kurucz (1993). An arbitrary constant shift was applied to each object for convenient comparision. The magnitude scale (Y-axis) is held identical for all panels.

magnitude range is essentially identical. The positions of the circles represent the central peak wavelength of the BATC filters. We can distinguish hot BHB stars and cool RGB or AGB stars either from their SEDs or directly from the corresponding effective temperature. The comparison in Figure 4 indicates that there are no systematic differences between our observations and the Kurucz model as a function of wavelength, similar to the finding in Clampitt & Burstein (1997). In Figure 4(*a*), we distinguish between the brightest stars in our sample ($m4 < 17$; *closed circles*) and fainter stars ($17 < m4 < 18$; *open circles*). It is rather clear that the large scatter in the comparison of SEDs versus model for RGB stars comes from the faint objects. The RGB stars with $m4 < 17$ have a range of S with wavelength similar to the bright AGB and BHB stars.

The primary goal of the BATC survey, as described in the previous section, is to establish accurate SEDs to sift galaxies, QSOs, AGNs, and peculiar objects from normal stars. At the same time, the low-dispersion spectra or SEDs would also be able to identify the high–red shift quasars. In this study, our central objective is to establish an accurate SED data bank using well-known properties of stars in star clusters to evaluate the efficiency and the accuracy of such a "sieve" process. The value of S from the least-squares fit to Kurucz models is an efficient way to screen nonstellar objects and field stars from the cluster members.

For cluster members, the average standard deviation value S is less than 0.05 (see Fig. 2). Thus, nonmembers, variable stars, and peculiar objects can be readily isolated from normal members of the clusters. Using the same technique, galaxies, QSOs, and AGNs can be easily separated from normal stellar SEDs. Hydra spectra were obtained using WIYN telescope at KPNO in 1998 August as a follow-up observation to inspect the nature of the objects with large S. Most of these peculiar objects have now been identified as white dwarfs, field giants, and subgiants. These data will be discussed elsewhere.

2.2. *Distance Modulus*

Comparison of observational data with the theoretical isochrones can provide valuable information such as distance, abundance, reddening, and age of stellar clusters. The limiting magnitude of this study is not deep enough to reach the main-sequence turnoff point of NGC 288, hence our data do not constrain the age of this cluster. Similarly, as we will show, the zero-point uncertainty in our spectrophotometry precludes an accurate estimate of reddening for this cluster. Rather, our discussion will concentrate on the distance modulus of the cluster, as well as provide a cross-check on our [Fe/H] estimate from the stellar SEDs (§ 2.3).

Isochrones calibrated in age and [Fe/H] have been kindly calculated by Guy Worthey for our BATC filter set, based on the Dial-a-Padova model of single-burst populations (Worthey 1994; Bertelli et al. 1994). From the studies of Bergbusch (1993) and Harris (1996), we choose the age 15 Gyr for NGC 288 and sample isochrones with [Fe/H] from -1.2 to -1.6 (Fig. 5). The primary distance indicator used to estimate distance for globular clusters is the mean V magnitude of the horizontal branch (or of the RR Lyrae stars), $V_{\rm HB}$. Wherever possible, the HB level is measured directly from a color-magnitude diagram (CMD);

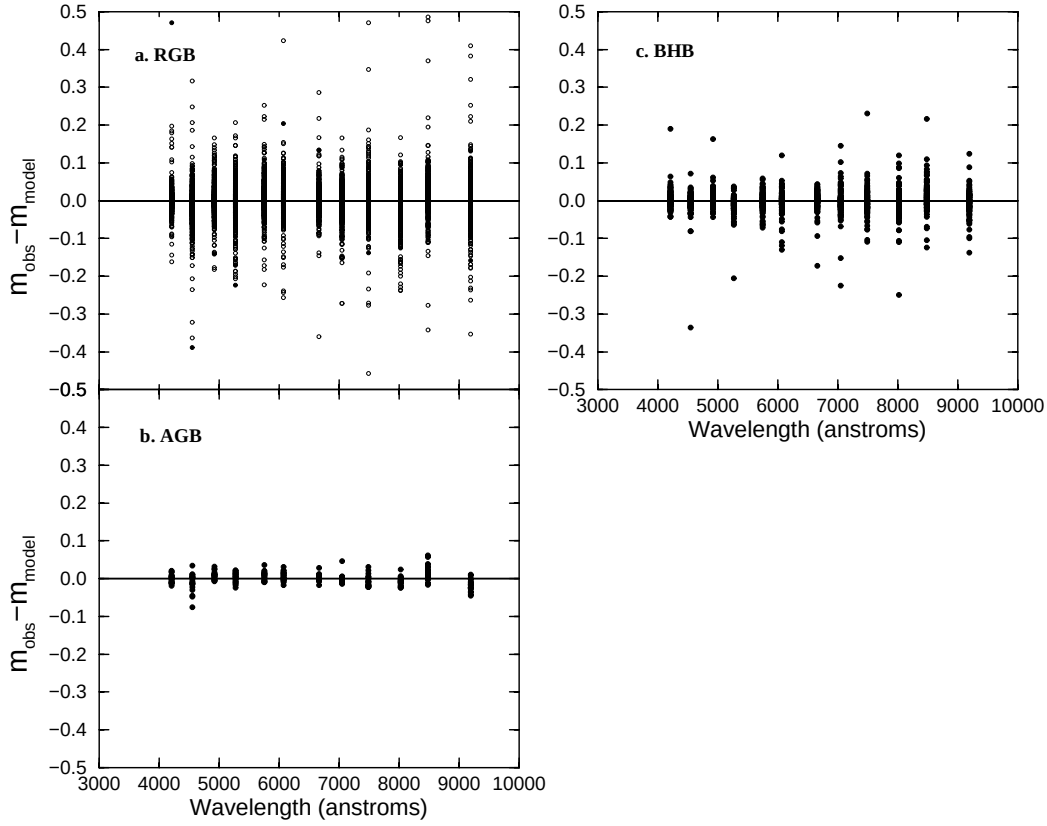

FIG. 4.—S ($m_{\rm obs} - m_{\rm model}$) vs. wavelength for stars with $m7 < 18$ for (*a*) RGB stars, (*b*) AGB stars, and (*c*) BHB stars. The objects for which $17 < m7 < 18$ are plotted as open circles in panel (*a*) to show that the large scatter for RGB stars is due to the fainter objects. Note the lack of any systematics between the BATC SEDs and the Kurucz models.

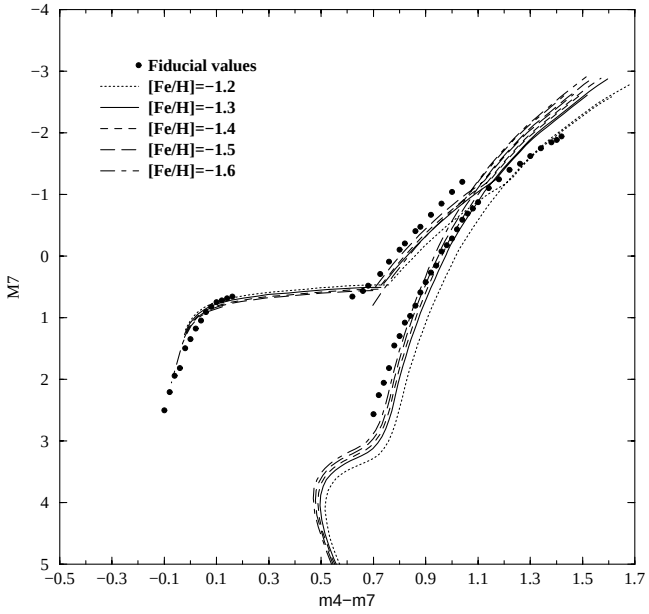

FIG. 5.—Isochrones for a 15 Gyr–old stellar population having the range of metallicities indicated, based on the calculations of G. Worthey, compared with the mean absolute observational AGB, RGB, and BHB (*circles*) in the $M7$ vs. $m4-m7$ diagram, as derived from our data for NGC 288. Based on this comparison, we obtain a distance modulus for NGC 288 of $m-M = 14.57 \pm 0.07$.

in a few cases for which CMDs are not yet available it can be evaluated from single-color photometry of the RR Lyrae variables or more roughly predicted from the magnitude of the brightest red giants. After detailed inspection, almost no RR Lyrae stars were observed or identified in this study. Thus the red end of the BHB was chosen to determine $m_{\rm HB}$ (Harris catalog[4]), yielding $(m-M)_{\rm HB} = 14.57 \pm 0.07$. This result is within 2 σ of the distance modulus value (14.69) cited in the most recent compilation by Harris.[4]

The reddening value $E(B-V)$ based on the DIRBE/IRAS map (Schlegel, Finkbeiner, & Davis 1998; hereafter SFD98) was derived in this direction and yields $E(B-V)_{\rm SFD98} = 0.0123$. This contrasts with the value $E(B-V) = 0.03$ cited by Harris.[4] An estimate of $E(m4-m7)$, our closest analog to $E(B-V)$, can be made by adopting the procedure suggested in Appendix B of SFD98. From a combination of known transmission curves of BATC filters, atmospheric transparency of Cerro Tololo, and Q.E. response of the Tektronix 2K CCD, we obtain

$$E(m4-m7) = 1.127E(B-V)\ . \qquad (1)$$

This relation yields the prediction $E(m4-m7)_{\rm SFD\,98} = 0.0139$.

RGB and BHB stars within the range $16 < m < 17$ are selected as the reddening calibrators from fitting $(m4-m7)_{\rm obs}$ and $(m4-m7)_{\rm iso}$, where "iso" indicates "isochrone." The best fit suggests $E(m4-m7) = 0.020 \pm 0.010$, equivalent to $E(B-V) = 0.018$ by equation (1). As all of these values are less than the photometric zero-point accuracy of our present data (0.06), we conclude that our data are consistent with all existing estimates of reddening for NGC 288.

There is still a discrepancy in the RGB, separate from errors in distance and reddening, that stems from a mismatch in slope between the models and the data among different parts of the CMD. The slope of the theoretical RGB favors more metal-rich isochrones, but the overall residual favors more metal-poor isochrones. There are two possibilities to explain this difference. The most likely is that the current isochrone models are not yet optimum for the upper RGB and AGB of globular clusters (Worthey 1994).

2.3. *Metallicity and Abundance*

The accuracies of metallicities and abundances obtained from comparing SEDs of stars with theoretical models are due to a combination of observational error and the finite grid of the models. We can overcome the finite metallicity resolution of the Kurucz models by estimating [Fe/H] for as many stars as possible.

In this analysis, we selected 792 members of NGC 288 ($m4 < 18$) for further study of cluster abundance. The histograms of [Fe/H] for RGB, AGB, and BHB are shown in Figure 6. The distribution of [Fe/H] is approximately concentrated at a value of [Fe/H] $= -1.21$. It should be noted, that there only 21 stars in AGB compared with 654 RGB stars. It appears that there is no clear peak in [Fe/H] for BHB, which suggests they are not very sensitive to SED modeling in abundance and thus are not suitable for determining abundance. This phenomenon implies that the selection of BHB as the fine calibrator in the previous section is reasonable and coincides with the isochrones. It should be mentioned that this, however, does not suggest that the theoretical SEDs from models are not working for the BHB, since the fit between models and observed SEDs yield an equally very small standard deviation.

We divided the RGB stars into three magnitude bins: $m4 < 16$, $16 < m4 < 17$, and $17 < m4 < 18$ and saw how the magnitude affects the abundance distribution (Fig. 7). It is rather clear that the number of stars in each magnitude bin increases steadily in the faint magnitudes, while the peak distribution of [Fe/H] remains nearly identical. However, dispersion of [Fe/H] increases dramatically toward the fainter end; perhaps with increasing contamination of field stars and main-sequence stars these cannot be separated because of the large scatter. As we have pointed out earlier, the giant-branch cutoff and MS begin at about $m7 \sim 17$–18. Furthermore, the abundance [Fe/H] for MS stars of NGC 288 is between -4 and -5. Thus, MS stars and perhaps also field objects start to appear.

After the above experiments, we find that the 170 stars with $m7 < 16$ (21 AGB stars and 149 RGB stars) yield the most accurate estimate of [Fe/H]. The estimated [Fe/H] values for these stars are shown in Figure 8 and yield [Fe/H] $= 1.24 \pm 0.04$. This result agrees well with previous studies (Harris catalog;[4] Shetrone & Keane 2000).

2.4. *Temperature and Color Index*

It was shown in § 2.1 that effective temperature can be derived by comparing observed SEDs with theoretical SEDs. In principle, a judicious choice of a sensitive color index can present this physical quantity, such as $B-V$ in the Johnson system and $b-y$ in the Strömgren system. We would like to correlate our BATC data with existing data, so that one color is close to $B-V$. In Table 1, $m4$ and $m7$ are the bandpasses that meet this criterion.

The relationship between $\log(T_{\rm eff})$ and $m4-m7$ for $m7 < 18$ is shown in Figure 9*a*. At $m4-m7 > 0$ the correlation between $\log(T_{\rm eff})$ and $m4-m7$ is nearly linear. However, at $m4-m7 < 0$, $T_{\rm eff}$ exponentially increases as

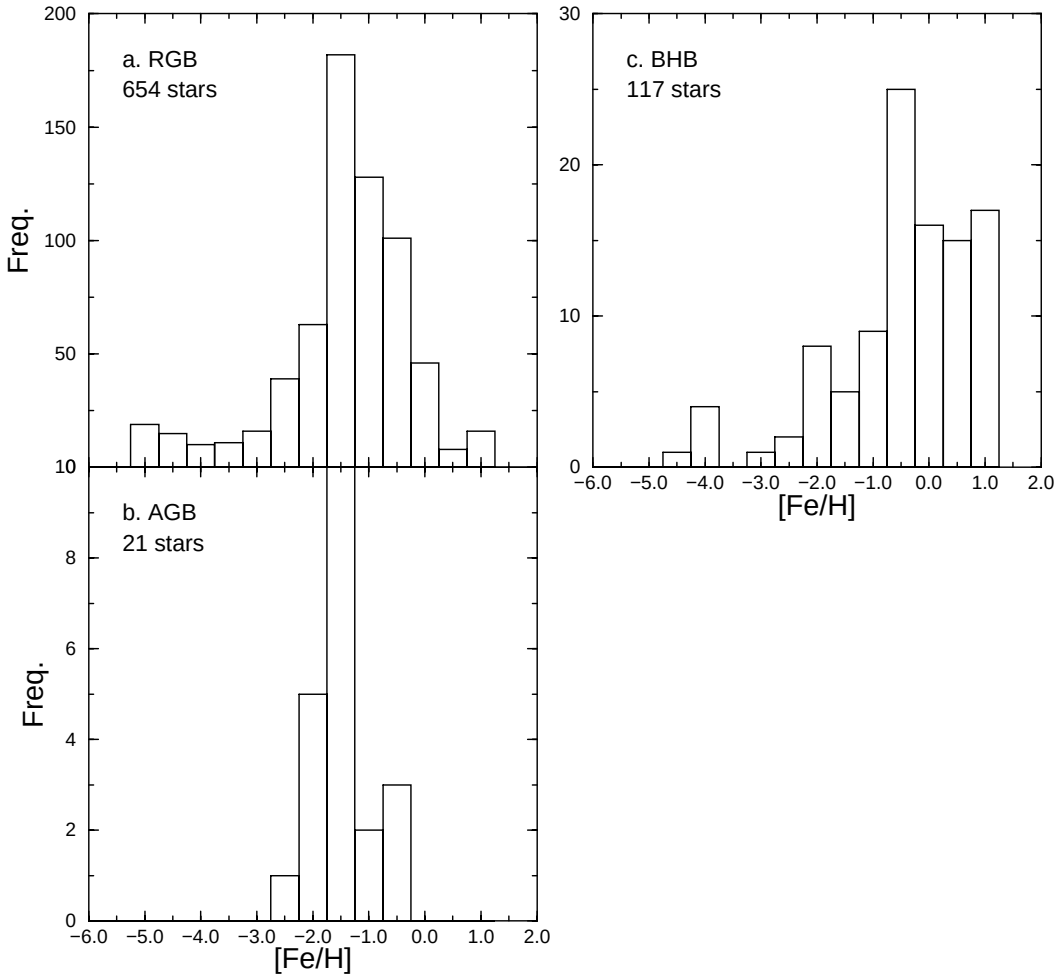

FIG. 6.— [Fe/H] histogram distribution for Kurucz-predicted metallicities for RGB, AGB, and BHB stars

$m4-m7$ becomes bluer. The relation between $T_{\rm eff}$ and color becomes vertical for the blue region $m4-m7 < -0.2$; therefore we have no temperature resolution for bluer $m4-m7$ colors.

To complement the $m4-m7$ color, we combine the $m3$ and $m4$ observations with those of the reddest filters used here ($m13$ and $m14$), as shown in Fig. 9*b*–9*e*. As can be seen here, one can define a simple polynomial relationship that well describes the relationship between log ($T_{\rm eff}$) and color indexes. In the future, when we have SEDs for stars with a wider range of age and abundance, we can use the full SEDs to define not only the temperatures of stars but also their gravity and abundance.

TABLE 4

NUMBER OF STARS AND σ FOR EACH REGION OF COLOR INDEXES

Color Index	Blue	Red	$\sigma_{\rm blue}$	$\sigma_{\rm red}$	$\sigma_{\rm overall}$
$m4-m7$	49	647	0.0378	0.0190	0.0208
$m3-m13$.....	101	667	0.0486	0.0125	0.0211
$m4-m13$.....	102	663	0.0551	0.0133	0.0236
$m3-m14$.....	90	616	0.0224	0.0117	0.0135
$m4-m14$.....	89	617	0.0242	0.0095	0.0124

NOTE.—The selection of blue and red regions for $m4-m7$ is the difference from the other four-color indexes: the blue region for $m4-m7$ is $-0.2 < m4-m7 < 0.1$, and the red region covers $0.1 < m4-m7 < 1.5$.

To help us in our future studies, however, it is valuable to define polynomial relationships between log ($T_{\rm eff}$) and our filter colors. To do so we separated the stars into two regions: the blue region covered the range of color index from -1.5 to -0.5, and the red region covered -0.5 to -2.5. Hot stars with log ($T_{\rm eff}$) > 4.3 were excluded from the fit. A quadratic polynomial

$$\log (T_{\rm eff}) = A + B({\rm CI}) + C({\rm CI})^2 , \qquad (2)$$

where CI is the color index, was adopted as the fitting function. The number of stars and σ for each region are listed in Table 4. It is rather clear that $m4-m14$ (Fig. 9*e*) gives us linearity in both the red and blue regions with the smallest

TABLE 5

COEFFICIENTS OF THE COLOR INDEX AND EFFECTIVE TEMPERATURE RELATION

Color Index	*A*	*B*	*C*
$m4-m14$, blue region.....	3.8546 ± 0.0045	0.0337 ± 0.0302	0.3604 ± 0.0118
$m4-m14$, red region.....	3.8443 ± 0.0001	-0.1430 ± 0.0001	0.0151 ± 0.0001

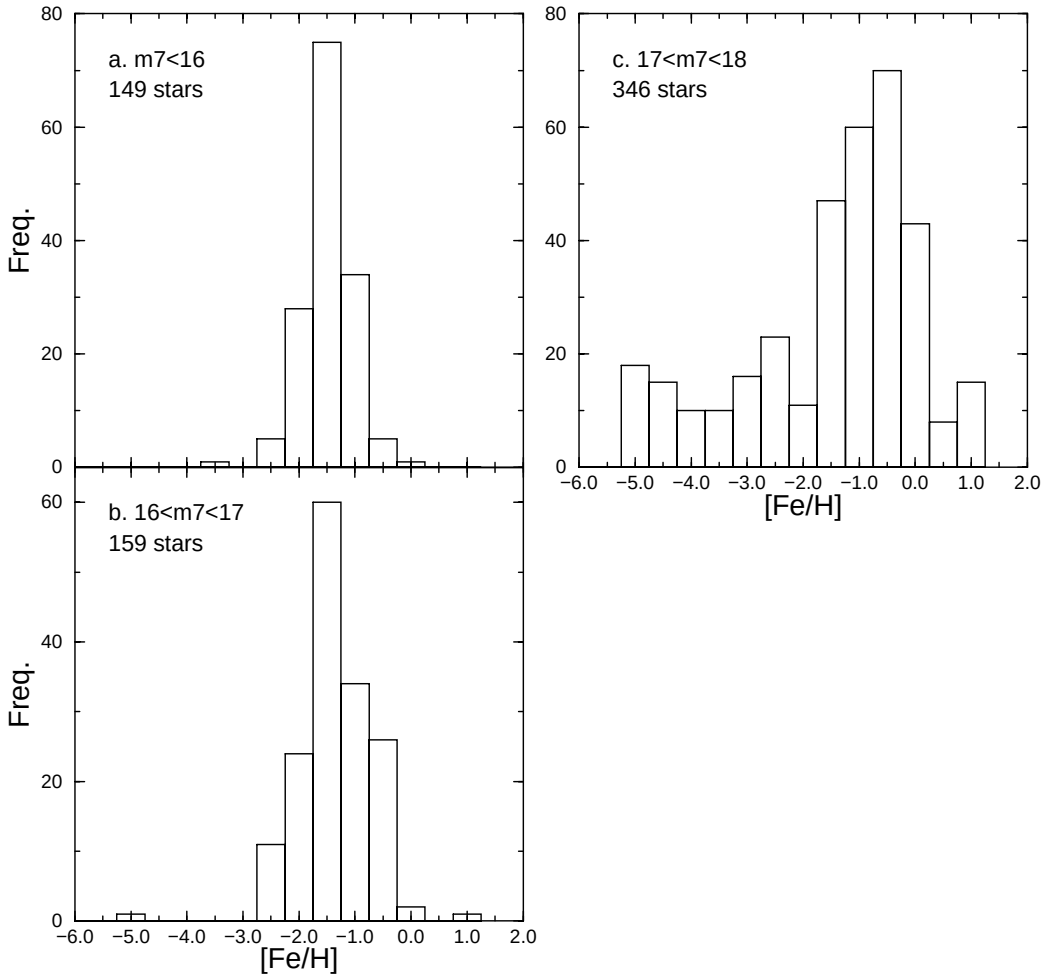

FIG. 7.— [Fe/H] histogram distribution for Kurucz-predicted metallicities of 654 RGB stars in different magnitude bins

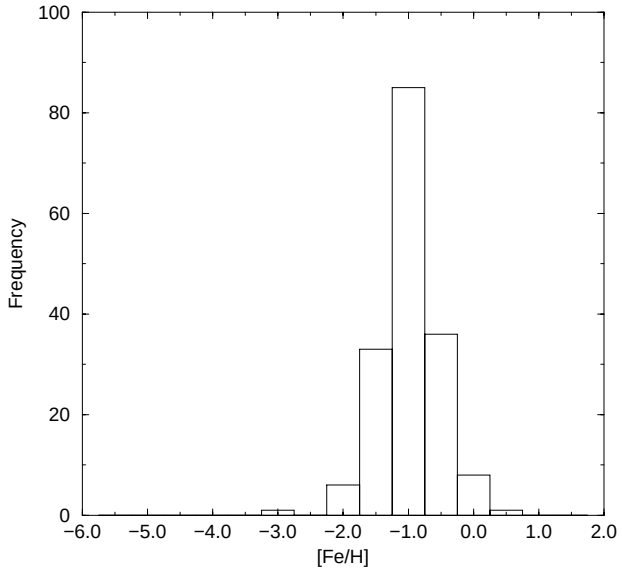

FIG. 8.— [Fe/H] histogram distribution for Kurucz-predicted metallicities for 21 AGB stars and 149 RGB stars with $m7 < 16$. These data yield [Fe/H] $= 1.24 \pm 0.04$.

scatter. The coefficients of equation (2) for $m4-m14$ are listed in Table 5.

3. RESULT AND SUMMARY

This study has used CCD intermediate-band filter observations of stars in the globluar cluster NGC 288 to produce a set of stellar spectral energy distributions (SEDs) that are well calibrated in terms of age, metallicity and temperature. To do this, we employed a combination of Kurucz theoretical SEDs for individual blue horizontal branch, red giant branch, and asymptotic giant branch stars in this cluster. Table 6 lists our results for the age and distance, together with all previously published data for this well-studied globular cluster. Our main results are the following:

1. From the comparsion of the SEDs for AGB and bright RGB stars with Kurucz model SEDs, we obtained an average value of [Fe/H] $= 1.24 \pm 0.04$ for this cluster.
2. From matching the theoretical isochrones (kindly calculated for us by G. Worthey) to the $m7$ versus $m4-m7$ color-magnitude diagram, we obtain a distance modulus for the cluster of $(m-M)_{HB} = 14.57 \pm 0.07$.
3. The most temperature-sensitive color index in our

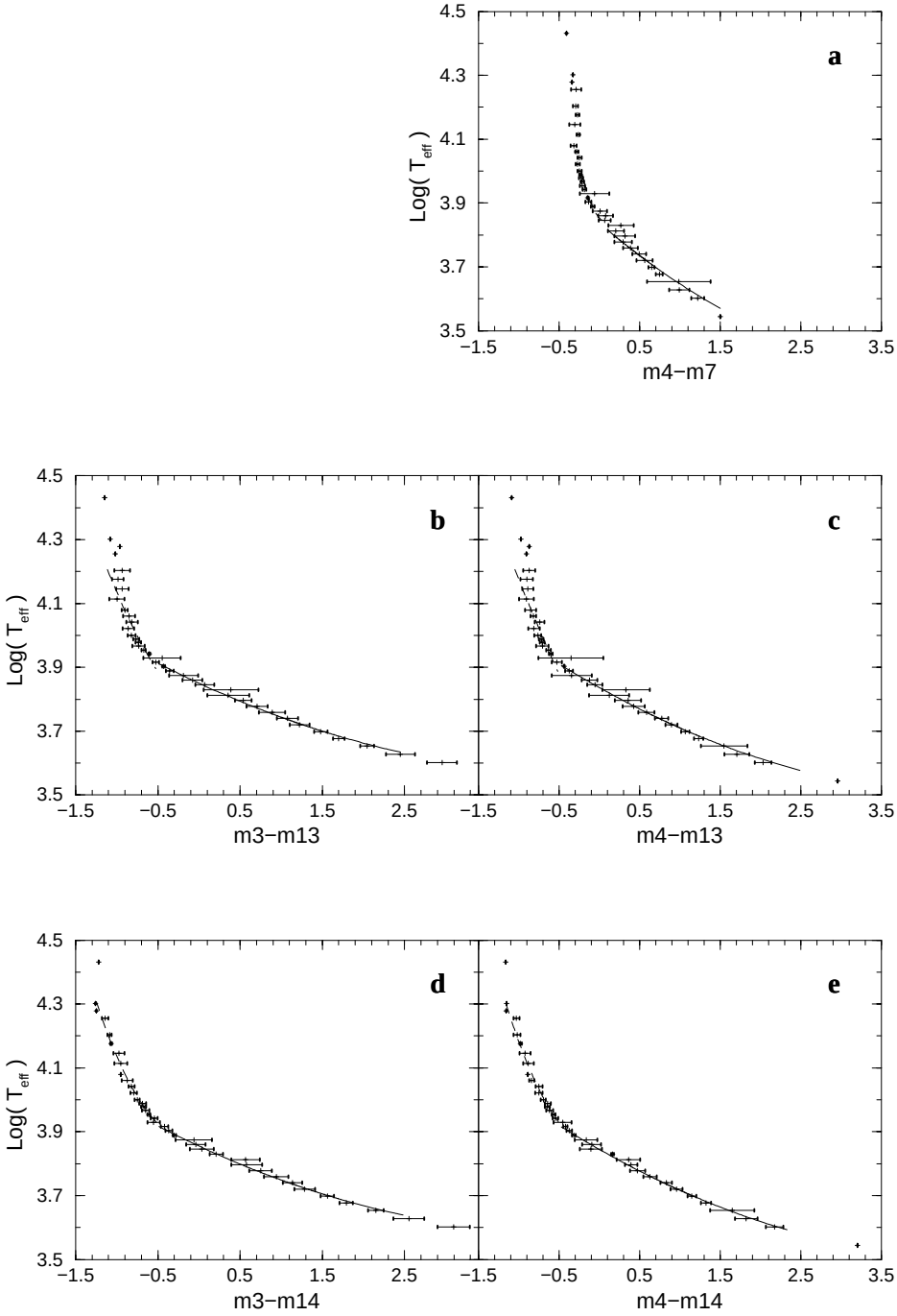

FIG. 9.—(*a*) Relationship of the $m4-m7$ color analog to $B-V$ with Kurucz model–predicted log ($T_{\rm eff}$). The relationship between log ($T_{\rm eff}$) and the color defined by the widest range of bandpasses in our data for (*b*) $m3-m13$, (*c*) $m4-m13$, (*d*) ($m3-m14$), and (*e*) $m4-m14$. Only stars with $m7 > 18$ are shown in these diagrams. The error bars were plotted based on $1-\sigma$ of color distribution in each temperature step of the Kurucz model.

study, $m4-m14$, was found to yield a well-defined empirical quadratic relation with log ($T_{\rm eff}$).

4. Perhaps most importantly, we show with these data that multicolor observations using the BATC system can accurately and conveniently be used to assess stellar temperature abundance and, possibly, gravity.

As pointed out in Section 2.1, we have confirmed the fact that the BATC SEDs can successfully separate field stars from cluster stars using spectra. In future papers in this series we will use the BATC filter system to study the SEDs of other open cluster and globular cluster stars.

We wish to thank Malcolm Smith and his staff at CTIO for their support. We are indebted to David Burstein at Arizona State University for his advice and guidance throughout this study. Thanks are also due to Guy Worthey at St. Ambrose University for his assistance in the theoretical modeling of isochrones and to William van Altena and John Lee at Yale for their collaboration in obtaining Hydra spectra using the WIYN telescope at KPNO. This research is partially supported by grants from the National Science Council to W. S. T. (NSC87-2112-M-008-026, NSC88-2112-M-008-032) and from the Perking Fund (CSU/AAUP) and from NSF to P. K. L.

TABLE 6

DISTANCE MODULUS, $E(B-V)$, [Fe/H], AND AGE FROM PREVIOUS STUDIES

Authors	$m-M$	$E(B-V)$	[Fe/H]	Age (Gyr)	Notes[a]
Cannon 1974	14.6	0.04 ± 0.03	...	...	P
Alcaino 1975	14.80 ± 0.03	0.05	Median	...	P
Alcaino & Liller 1980	14.70 ± 0.15	0.02 ± 0.02	-1.6	14.5 ± 2.5	P
Pilachowski & Sneden 1983	...	0.02 ± 0.02	-1.0 ± 0.2	...	S
Buonanno 1984a	...	0.02	-1.4	16 ± 3	P
Buonanno 1984b	...	0.02 ± 0.02	-1.3	16 ± 3	P
Penny 1984	14.92 ± 0.20	0.00	-1.0	16 to 17	P
Olszewski, Harris, & Canterna 1984	14.6	0.03 ± 0.01	-1.3	15 ± 3	P
Alcaino, Liller, & Alvarado 1987	...	0.0	-1.41	...	P
Montgomery and Janes 1994, 136	14.55 ± 0.20	0.03	-1.3 ± 0.1	...	P
Caldwell & Dickens 1988	14.5	0.03	-1.0	...	S
Bolte 1989	14.7	0.015	...	...	P
Green & Norris 1990	14.71	0.015	-1.2	...	P
Pryor et al. 1991	15.3	0.04	-1.3	...	P
Bergbusch 1993	14.90	0.03	-1.26	14	P
Kaluzny 1996	14.71	...	-1.4	...	P
Chen 1996	14.9 ± 0.2	0.03	...	15 ± 3	P
Alcaino et al. 1997	14.85 ± 0.10	0.04 ± 0.02	-1.26	14 ± 2	P
Harris 1999	14.69	0.03	-1.24	...	
Shetrone & Keane 2000	...	...	-1.39 ± 0.01	...	S
Chen et al. (this study)	14.57 ± 0.07	0.018 ± 0.010	-1.24 ± 0.04[b]	...	P

[a] (P) photometry; (S) spectroscopy.
[b] For RGB and AGB stars with $m7 < 16$.

REFERENCES

Alcaino, G. 1975, A&AS, 21, 15
Alcaino, G., & Liller, W. 1980, AJ, 85, 1592
Alcaino, G., Liller, W., & Alvarado, F. 1987, AJ, 93, 1464
———. 1997, AJ, 114, 2626
Bergbusch, P. A. 1993, AJ, 106, 1024
Bertelli, G., Bressan, A., Choiso, C., Fagotto, F., & Nasi, E. 1994, A&AS, 106, 275
Bolte, M. 1989, AJ, 97, 1688
Buonanno, R., Corsi, C. E., Fusi-Pecci, F., Alcaino, G., & Liller, W. 1984a, A&AS, 57, 75
Buonanno, R., Corsi, C. E., Fusi-Pecci, F., Liller, W., & Alcaino, G. 1984b, ApJ, 277, 220
Caldwell, S. P., & Dickens, R. J. 1988, MNRAS, 234, 87
Cannon, R. D. 1974, MNRAS, 167, 551
Chen, R. 1996, Ph.D. thesis, Institute of Astronomy, National Central University, Chung-Li, Taiwan
Clampitt, L., & Burstein, D. 1997, AJ, 114, 699
Deng, L., Chen, R., Liu, X. S., & Chen, J. S. 1999, ApJ, 524, 824
Fan, X. H., et al. 1996, AJ, 112, 628
Green, E. M., & Norris, J. E. 1990, ApJ, 353, 17L
Gunn, J. E., & Stryker, L. 1983, ApJS, 52, 121
Guo, X., Girard, T. M., van Altena, W. F., & Lopez, C. E. 1993, AJ, 105, 2182
Harris, W. E. 1996, AJ, 112, 1487
Kaluzny, J. 1996, A&AS, 120, 83
Kurucz, R. L. 1993, CD-ROM 13, ATLAS9 Stellar Atmosphere Programs and 2km/s Grid (Cambridge: Smithsonian Astrophys. Obs.)
Lee, Y. W., Demarque, P., & Zinn, R. 1990, ApJ, 350, 155
Lu, P. K. 1989, in The Gravitational Force Perpendicular to the Galactic Plane, ed. A. G. D. Philip & P. K. Lu (Schenectady: L. Davis)
Lu, P. K. 1991, in The Objective-Prism and Other Surveys, ed. A. G. D. Philip & A. R. Upgren (Schenectady: L. Davis)
———. 1993, in Workshop on Databases for Galactic Structure, ed. A. G. D. Philip, B. Hauck, & A. R. Upgren (Schenectady: L. Davis)
Lu, P. K., Miller, J., & Platt, D. 1992, ApJS, 83, 203
Lu, P. K., Tsay, W. S., & Chen, A. 1999, in The Anni Mirabiles: A Symposium Celebrating the 90th Birthday of Dorrit Hoffleit, ed. A. G. D. Philip, W. F. van Altena, & A. R. Upgren (Schenectady: L. Davis)
Lu, P. K., et al. 1997, Baltic Astron., 6, 33
Montgomery, K. A., & Janes, K. A. 1994, in The Hot Stars in the Galactic Halo, ed. S. Adelman, A. R. Upgren, & C. Adelman (Cambridge: Cambridge Univ. Press)
Oke, J. B., & Gunn J. E. 1983, ApJ, 266, 713
Olszewski, W. E., Harris, W. E., & Canterna, R. 1984, ApJ, 281, 158
Penny, A. J. 1984, MNRAS, 208, 559
Pilachowski, C. A., & Sneden, C. 1983, PASP, 95, 229
Platais, I., et al. 1998, AJ, 116, 2556
Pryor, C., McClue, R. D., Fletcher, J. M., & Hesser, J. E. 1991, AJ, 102, 1026
Schlegel, D. J., Finkbeiner, D. P., & Davis, M. 1998, ApJ, 500, 525
Shetrone, M. D., & Keane, M. J. 2000, AJ, 119, 840
Stetson, P. B. 1987, PASP, 99, 191
Stetson, P. B., Vandenberg, D. A., & Bolte, M. 1996, PASP, 108, 560
Tsay, W. S., Chen, A., Lu, P. K., Smith, A., & Mendez, R. 1997, Baltic Astron., 6, 141
van den Bergh, S., & Hesser, J. E. 1993, Sci. Am., 268, 72
Worthey, G. 1994, ApJS, 95, 107
Zheng, Z. Y., et al. 1999, AJ, 117, 2757